Mechanisms of Ageing and Development 191 (2020) 111328

Contents lists available at ScienceDirect

Mechanisms of Ageing and Development

journal homepage: www.elsevier.com/locate/mechagedev

Prolonged hypoxia delays aging and preserves functionality of human amniotic fluid stem cells

Francesca Casciaro [a,b,c], Michela Borghesan [a], Francesca Beretti [b], Manuela Zavatti [b], Emma Bertucci [d], Matilde Yung Follo [c], Tullia Maraldi [b], Marco Demaria [a,*]

[a] University of Groningen, European Research Institute for the Biology of Ageing (ERIBA), University Medical Center, Groningen (UMCG), The Netherlands
[b] Department of Surgical, Medical, Dental and Morphological Sciences With Interest in Transplant, Oncology and Regenerative Medicine, University of Modena and Reggio Emilia, Italy
[c] Cellular Signalling Laboratory Department of Biomedical and Neuromotor Sciences, University of Bologna, Bologna, Italy
[d] Department of Medical and Surgical Sciences for Mothers, Children and Adults, University of Modena and Reggio Emilia, Azienda Ospedaliero Universitaria Policlinico, Modena, Italy

ARTICLE INFO

Keywords:
Aging
Amniotic fluid stem cells
Cellular senescence
Hypoxia
Mesenchymal stem cells
Oxygen
Stem cells
Senescence pluripotency

ABSTRACT

Human amniotic fluid stem cells (hAFSCs) are an emerging tool in regenerative medicine because they have the ability to differentiate into various lineages and efficiently improve tissue regeneration with no risk of tumorigenesis. Although hAFSCs are easily isolated from the amniotic fluid, their expansion *ex vivo* is limited by a quick exhaustion which impairs replicative potential and differentiation capacity. In this study, we evaluate various aging features of hAFSCs cultured at different oxygen concentrations. We show that low oxygen (1% O_2) extends stemness and proliferative features, and delays induction of senescence-associated markers. Hypoxic hAFSCs activate a metabolic shift and increase resistance to pro-apoptotic stimuli. Moreover, we observe that cells at low oxygen remain capable of osteogenesis for prolonged periods of time, suggesting a more youthful phenotype. Together, these data demonstrate that low oxygen concentrations might improve the generation of functional hAFSCs for therapeutic use by delaying the onset of cellular aging.

1. Introduction

Transplantation of mesenchymal stem cells (MSCs) has emerged as a potential therapeutic approach to treat or delay various disorders (Wang et al., 2012). MSCs are present in foetal and adult tissues with variable levels of accessibility, and in the last years more interest has been focused toward the amniotic fluid (AF). A major advantage of AF-MSCs over adult MSCs, such as bone marrow-derived mesenchymal stem cells (BM-MSCs), is their minimally invasive isolation procedure. AF can be collected early during pregnancy, *via* routine amniocentesis (from 16 weeks of gestation), and includes various cell types, like progenitors/undifferentiated cells. Among those, CD117-expressing (c-kit) stem cells (hAFSCs) comprise at least 1% of the total cellular population and proliferates rapidly with clonal lines having a doubling time of 36 h. hAFSCs express pluripotent markers (Antonucci et al., 2014) and have the ability to differentiate into mesodermal and non-mesodermal lineages under appropriate differentiation conditions (Ullah et al., 2015a). Importantly, hAFSCs, unlike embryonic stem cells or induced pluripotent stem cells (IPS), do not form neither tumors *in vivo* nor chimeras when injected into blastocysts (Roubelakis et al., 2007). Moreover, hAFSCs present a low immunogenic profile due to expression of antigens belonging to the MHC-I (HLA- A, B and C), but not of the MHC-II (HLA-DR) class (Cananzi and De Coppi, 2012).

For these reasons, AFSCs can serve as an autologous stem cell source for pre- and postnatal regenerative medicine applications (Loukogeorgakis and De Coppi, 2016).

However, as for other types of MSCs, the number of hAFSCs isolated during amniocentesis remains low, and the purified population requires substantial *ex vivo* expansion prior to clinical use (Antoniou et al., 2004). This expansion can quickly lead to hAFSCs loss of differentiation

* Corresponding author at: European Research Institute of the Biology of Ageing, University Medical Center, A. Deusinglaan 1, 9713 AV Groningen, The Netherlands.
E-mail addresses: francesca.casciaro3@unibo.it (F. Casciaro), m.borghesan@umcg.nl (M. Borghesan), francesca.beretti@unimore.it (F. Beretti), manuela.zavatti@unimore.it (M. Zavatti), emma.bertucci@unimore.it (E. Bertucci), matilde.follo@unibo.it (M.Y. Follo), tullia.maraldi@unimore.it (T. Maraldi), PhDm.demaria@umcg.nl (M. Demaria).

https://doi.org/10.1016/j.mad.2020.111328
Received 10 April 2020; Received in revised form 7 August 2020; Accepted 9 August 2020
Available online 13 August 2020

capacity and exhaustion due to induction of cellular senescence. Cellular senescence is a process of irreversible growth arrest originally described in 1960s by Leonard Hayflick as the limiting proliferative potential of most cells (Hayflick, 1965). Cellular senescence naturally occurs as a consequence of the gradual shortening of telomeres deriving from continuous replication (Hernandez-Segura et al., 2018). Moreover, induction of senescence can be accelerated and prematurely induced by a number of environmental cues, including excessive oxidative stress (Davalli et al., 2016). The stable growth arrest associated to senescence is seen as a major mechanism leading to loss of regenerative potential (Krishnamurthy et al., 2006). During aging, multiple mechanisms are responsible for the decline of stem cells functionality. For example, alteration in the niche composition or accumulation of protein aggregates and dysfunctional organelles can induce metabolic changes, modification in the epigenetic pattern and DNA damage ultimately causing their aberrant proliferation and differentiation (Ermolaeva et al., 2018). As for hAFSCs, in general young mesenchymal stem cells are able to differentiate into mesodermal lineage such as osteocytes, adipocytes and chondrocytes as well as ectodermal (neurocytes) and endodermal lines (hepatocytes) (Ullah et al., 2015b).With aging, old MSCs show a biased differentiation towards adipogenesis at the expense of osteogenesis, a feature that correlates with the onset of osteoporosis (Coipeau et al., 2009). However, the effect of oxygen conditions on differentiation remains controversial and dependent on the cellular source and the differentiation protocol (Kim et al., 2014; Wagegg et al., 2012; Valorani et al., 2012).

hAFSCs, as most MSCs, are commonly expanded at atmospheric oxygen concentration (20 % O_2), which is sharply higher than the physiological concentration at which they normally reside in their natural niches (~2.3 % O_2) (Jauniaux et al., 1999). This higher oxygen tension might increase reactive oxygen species (ROS) levels and oxidative stress, eventually leading to premature senescence (Antoniou et al., 2004). MSCs cultured in hypoxic conditions (2% O_2) express lower levels of senescence-associated genes compared to cells cultured in normoxia and can generally undergo further expansion (Grayson et al., 2006), (Choi et al., 2014).

In addition, multiple studies have demonstrated that MSCs cultivated at low oxygen concentrations express higher levels of pluripotent and proliferation markers (Choi et al., 2014). This effect could be the consequence of two separate processes: on one side the expression of the pluripotent marker Oct4 might directly promote proliferation by suppressing the cyclin-dependent kinase inhibitor p21 [Lu et al., 2019] and by activating cyclin D1 through the binding the promoter region of miR-302a (Greer Card et al., 2008), which play a critical role in regulating G1-S transition (Gao et al., 2015). On the other side, low oxygen tensions are normally associated with reduced levels of double-strand breaks (DSB), chromosomal abnormalities, aneuploidy and telomere shortening rates (Li and Marbán, 2010; Estrada et al., 2012). Together with improved proliferation and pluripotency, cells cultured in hypoxia seem more resistant to undergo apoptosis, either spontaneously or under treatment with pro-apoptotic stimuli (Choi et al., 2014; Korski et al., 2019). However, other authors have reported discordant observations. For example, Pezzi et al. in 2017 found that hypoxia was insufficient to significantly perturb viability, immunophenotyping, differentiation and ROS levels in bone marrow-derived mesenchymal stem cells (Pezzi et al., 2017). An important technical aspect is that most studies have focused on the transient effect of hypoxic conditions on the phenotypical behaviour of stem cell (Kwon et al., 2017; Holzwarth et al., 2010), and a comprehensive characterization of prolonged exposure to low oxygen conditions is missing.

Here, we investigated which oxygen concentration counteracts the onset of aging phenotypes associated with stem cell exhaustion, with the purpose of implementing novel culturing conditions to allow the generation of sufficient functional hAFSCs to use in regenerative medicine.

2. Results

2.1. Stemness properties of hAFSCs are maintained under hypoxia

We initially isolated and purified c-kit$^+$ amniotic fluid stem cells and cultured at 20 % O_2, in accordance with standard procedures (see methods section). After 1 week of culture, cells were characterized for the expression of stemness and mesenchymal markers (Figure S1) and subsequently divided in three populations incubated at 20 %, 5% and 1% O_2, respectively. The three cell populations were maintained for 5 weeks in these conditions, and their stemness properties evaluated at different time points.

mRNA levels of Oct4 were increased in cells cultured 1% O_2 already at 1 week, and this upregulation was maintained until the end of the experiment (Fig. 1A). Oct4 upregulation was confirmed at the protein level both at 2 and 5 weeks of culture (Fig. 1 B-C). Importantly, elevated expression corresponded with an increased transcriptional activity, as measured by binding to a reporter gene (Fig. 1D) and by enhanced expression of the direct target genes ZNF462, ZNF219, RCOR2, SMARCC1, RIF1(Fig. 1E), reported to correlate with Oct4 expression and the maintenance of undifferentiated states (van den Berg et al., 2010). Even if not statistically significant, the same trend was observed also for SOX2. In contrast to Oct4 elevated expression, no significant differences in Nanog levels were observed (Figure S2).

Thus, to validate whether low oxygen tension favors stemness properties, we evaluated the protein expression of SSEA4, another hAFSCs stemness marker (Cananzi and De Coppi, 2012). SSEA4 was significantly upregulated in cells cultivated at 1% O_2 in comparison to cells at 20 % O_2 after 4 weeks of culture, as revealed by immunofluorescence analysis and quantification (Fig. 1F–G).

Altogether, these data suggest that hAFSCs cultured under hypoxic conditions maintain stemness properties for a prolonged period of time.

2.2. Proliferative ability of hAFSCs depends on oxygen tensions

Hypoxia generally stimulates cell cycle arrest in mammalian cells (Gardner et al., 2001). However, different studies reported that MSCs initially grow slower under 5% O_2 tension but acquire a growth advantage over time (Grayson et al., 2006). Similarly, the proliferative rate of 1% O_2 hAFSCs resulted slightly lower for the first 3 weeks of culture, but sharply increased afterwards, resulting in a significant increase in overall cell number in comparison to 5% and 20 % O_2 at both 4 and 5 weeks of culture (Fig. 2A). In accordance, DNA synthesis dropped in 20 % O_2 cells after 5 weeks of culture, while remaining stable in cells cultured at lower oxygen (Fig. 2B-2C).

Since, a previous study reported that higher Oct4 expression is associated with more cells entering S phase (Lee et al., 2010), we then measured the expression levels of the S-phase entry protein Cyclin E2 after 5 weeks of culture. Similarly to what observed in the proliferative rate, the protein levels of Cyclin E2 resulted upregulated in cells cultured at lower oxygen concentrations, with highest expression observed in cells at 1% O_2 (Fig. 2D and S3).

To further evaluate cell cycle progression, we measured the expression of Ki67, a proliferation marker which reaches its maximum during M phase (Mulyawan, 2019). Immunofluorescence analysis revealed higher expression of Ki67 in cells cultured for 5 weeks at 1% and 5% O_2 after 5 weeks of culture (Figure E and F).

Finally, we analysed the level of the PI3K/Akt pathway, a master regulator of cell proliferation shown to be activated in BM-MSCs under hypoxia (Sheng et al., 2017). Cells cultured at lower oxygen presented increased level of phosphorylated Akt after 5 weeks of culture, suggesting elevated activation (Fig. 2G-2 H).

Overall, these data suggest that hAFSCs cultured in low oxygen conditions maintain proliferative capacity for a prolonged period of time.

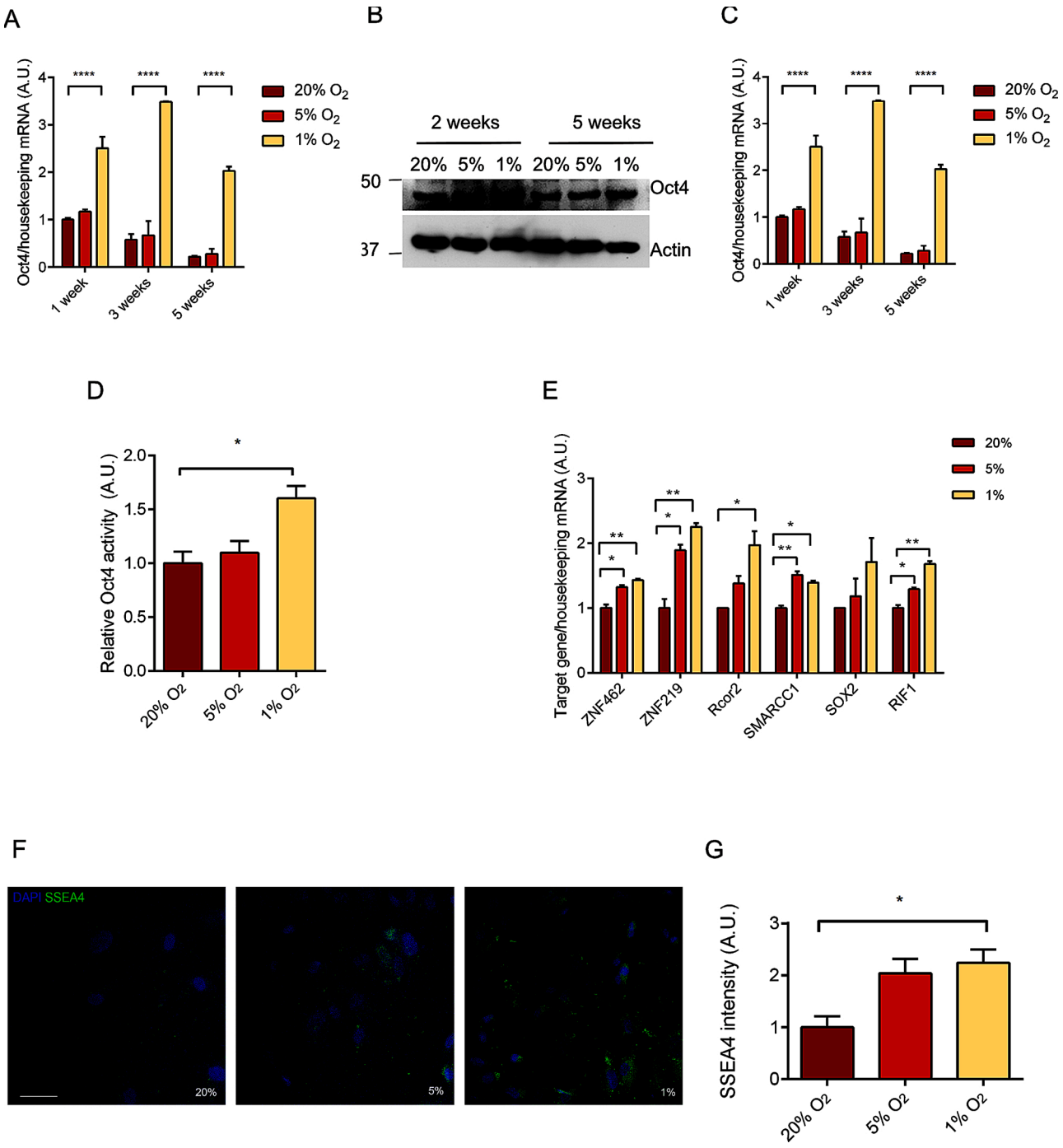

Fig. 1. hAFSCs stemness markers expression. A) Relative normalized expression of Oct4 in cells exposed to 20%, 5%, 1% oxygen tension. Tubulin and actin were used as housekeeping. ****p value < 0.0001 significantly different from 20%. B-C) Representative western blot (B) and its densitometric analysis (C) showing the expression of Oct4 in hAFSCs cultivated at different oxygen tensions. ***p value < 0.001; ****p value < 0.0001. D) Comparison of normalized activity of Oct4 between 20%, 5%, and 1% exposed cells measured after 10 days in culture. *p value < 0.05. E) Relative normalized expression of some Oct4 target genes. Tubulin and actin were used as housekeeping. *p value < 0.05; **p value < 0.01. F-G) Representative confocal microscopy images of SSEA4 stemness marker (green) are reported in F. Nuclei were stained with DAPI (blue). Scale bar =10 μm. Panel G shows the relative normalized expression of corrected total cell fluorescence of SSEA4 staining. *p value < 0.05. A.U.= arbitrary units. Numeric data are presented as Mean +/- SEM. Data were obtained analysing at least two of the four patients in each experiment.

2.3. Induction of senescence-associated markers in hAFSCs is delayed in hypoxia

Maintenance of proliferative potential might reflect a delay in the induction of replicative senescence.

Interestingly, we observed that prolonged culture of hAFSCs at 20 % O_2 resulted in senescence-like changes in cell size, in particular a bigger, flattened and partially elongated morphology (Fig. 3A, Figure S4). However, these morphological changes were not observed in cells cultured at 1% or 5% O_2.

Senescence-associated β-galactosidase (SAβgal) staining performed at 4 and 5 weeks of culture confirmed a higher percentage of senescent cells in the population cultured at 20 % O_2, particularly in comparison to cells at 1% O_2 (Fig. 3B–C). Similarly, expression of the two most

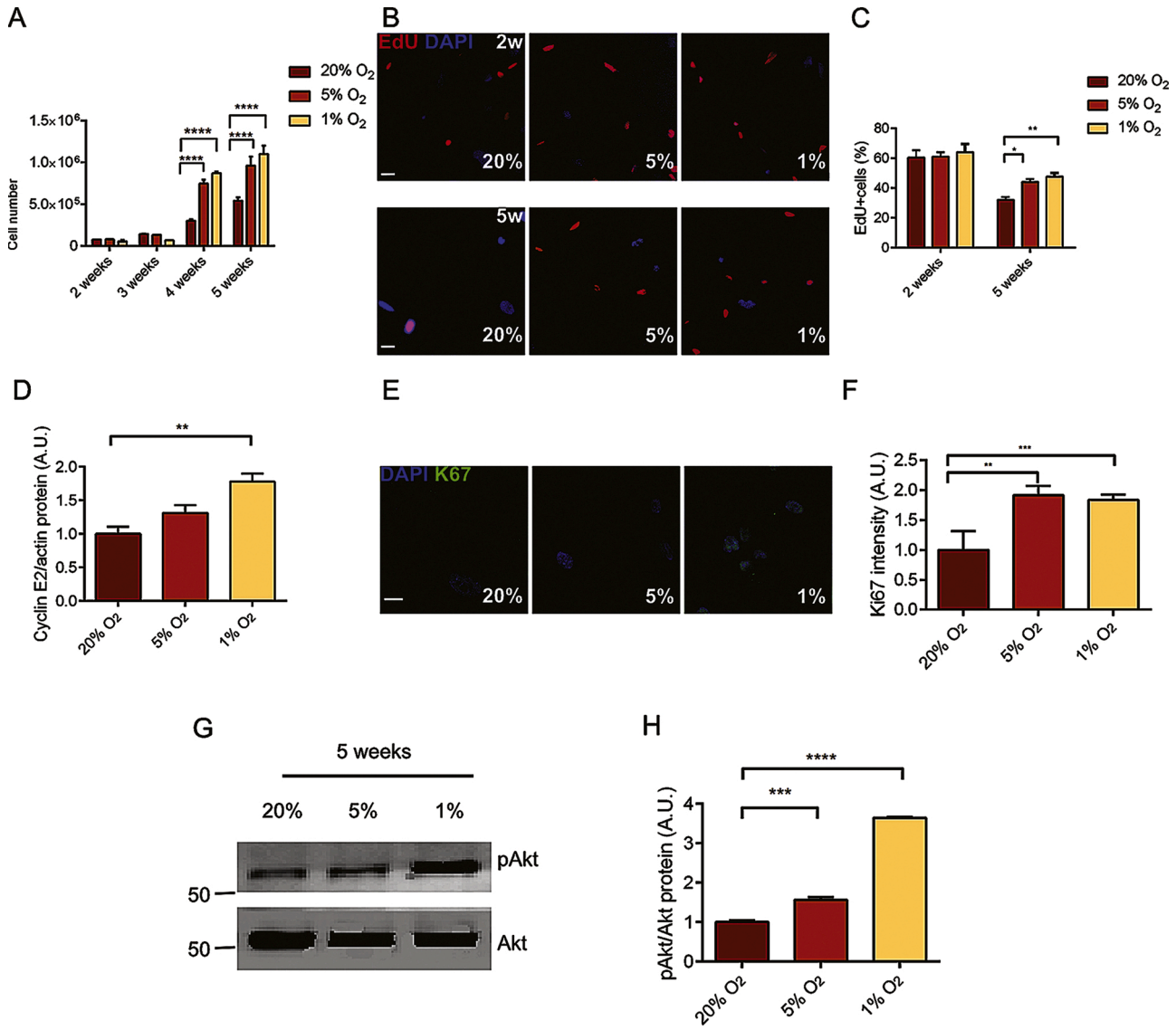

Fig. 2. Proliferation ability of hAFSCs cultivated at different oxygen tensions. A) Cellular growth of hAFSCs cultivated at 20%, 5% and 1% for 5 weeks. ****p value < 0.0001. B-C) EdU test showing proliferating cells (stained in red) performed after 2, 4 weeks, and 5 weeks of culture at 20%, 5% and 1% oxygen tension. Nuclei were stained with DAPI (blue). *p value < 0.05; **p value < 0.01. Scale bar =75 μm. D) Western Blot densitometry of Cyclin E2 levels in cells maintained at 20%, 5% and 1% oxygen tension after 5 weeks of culture. Actin was used as loading control. **p value < 0.01.E-F) Confocal images and relative normalized expression of corrected total cell fluorescence of Ki67 staining of hAFSCs cultivated at different oxygen tensions and marked with DAPI (blue) and Ki67 (green). Scale bar =10 μm; **p value < 0.01; ***p value < 0.001.G-H) Representative western blot image and relative densitometry analysing the ratio pAkt/Akt in hAFSCs cultivated at 20%, 5% and 1% oxygen tension after 5 weeks. ***p value < 0.001; ****p value < 0.0001. A.U.= arbitrary units. Numeric data are presented as Mean +/- SEM. Data were obtained analysing at least two of the four patients in each experiment.

important senescence-associated cell cycle inhibitors, p16 and p21 was reduced in 1% compared to 20 % O_2 as evaluated by transcript (Fig. 3D) and protein levels (Fig. 3E, F). However, only for p21 expression the data resulted significant.

We have previously observed that old hAFSCs accumulate prelamin A, the immature form of the nuclear lamina protein lamin A, which expression is associated with senescence-like features (Casciaro et al., 2018). In accordance with a delay in replicative senescence, cells at 1% and 5% O_2 expressed significantly lower level of prelamin A compared to cells at 20 % O_2 after 4 weeks of culture (Fig. 3G–H).

Another characteristic of aging in hAFSCs, is the accumulation of PML bodies, which are proposed to be involved in the regulation of stem cell self-renewal and cellular senescence (Casciaro et al., 2018; Salomoni and Pandolfi, 2002)

Immunofluorescent analysis revealed that cells at lower oxygen concentrations accumulated less and smaller PML bodies compared to cells at 20 % O_2 after 4 weeks of culture (Fig. 3I–J). In summary, the data presented here suggest that culturing hAFSCs in low oxygen conditions, and in particular in 1% O_2, is sufficient to delay the onset of replicative senescence.

2.4. Low oxygen tension induces changes in metabolism and results in increased resistance to stress

Metabolic adaptation to low oxygen conditions is an essential step for cellular survival. Lower oxygen availability activates anaerobic glycolysis and inhibits the mitochondrial aerobic metabolism, the tricarboxylic acid (TCA) cycle and OXPHOS (Solaini et al., 2010).

As expected, PDK1, which acts inactivating the TCA cycle, and Glut1, which is a glucose transporter essential to maintain elevated glucose uptake to support glycolysis, were gradually upregulated in hAFSCs in low oxygen conditions (Fig. 4A, B, C).

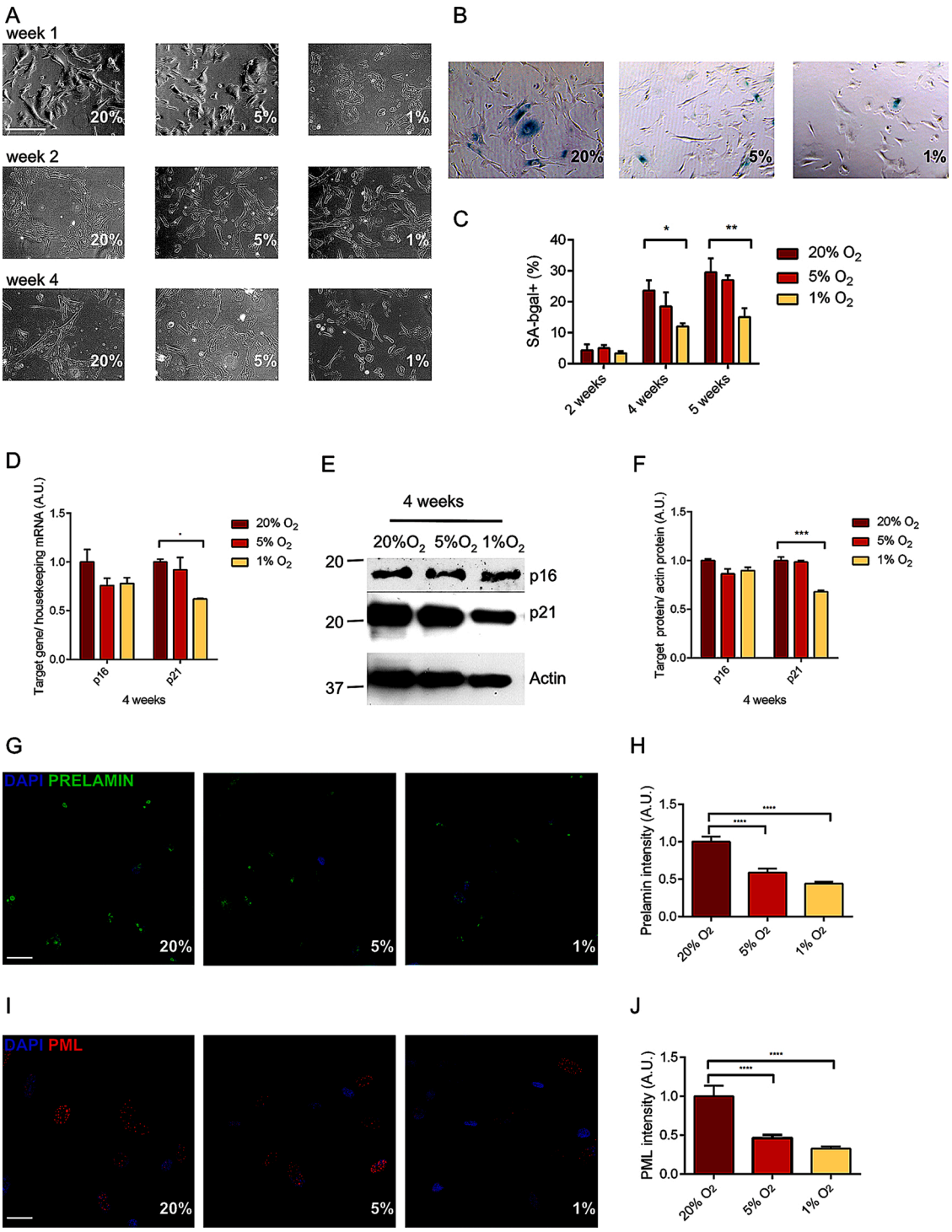

Fig. 3. Expression of senescence-associated markers at different oxygen tensions. A) Morphology of cells after 1, 2 and 4 weeks of cultivation at 20%, 5% and 1% oxygen tension. Scale bar =30 μm. B-C) Representative images of cells stained for SAbgal^{+} (B). Cells in blue are positive for the staining. Scale bar =30 μm. In panel C, evaluation of positive cells at SAbgal^{+} staining in hAFSCs cultivated at different oxygen tensions for 2,4,5 weeks. *p value < 0.05; **p value < 0.01. D) qPCR analysis for p16 and p21 expression in hAFSCs cultivated at 20%, 5% and 1% oxygen tensions. Tubulin and actin were used as housekeeping. *p value < 0.05. E-F) Representative image of p16 and p21 western blot analysis (E) and their densitometry (F). Values were normalized on actin expressions. ***p value < 0.001. G-H) Prelamin A expression (green) after 4 weeks of culture at different oxygen tensions. Nuclei were stained with DAPI (blue). Scale bar =10 μm. Panel H shows the relative normalized expression of corrected total cell fluorescence of prelamin A staining. ****p value < 0.0001. I-J) Representative confocal images of PML bodies (red) in hAFSCs cultivated at 20%, 5% and 1% oxygen tension. Nuclei were visualized with DAPI (blue). Scale bar =10 μm. The panel J reports relative normalized expression of corrected total cell fluorescence of PML bodies staining. ****p value < 0.0001. A.U.= arbitrary units. Numeric data are presented as Mean +/- SEM. Data were obtained analysing at least two of the four patients in each experiment.

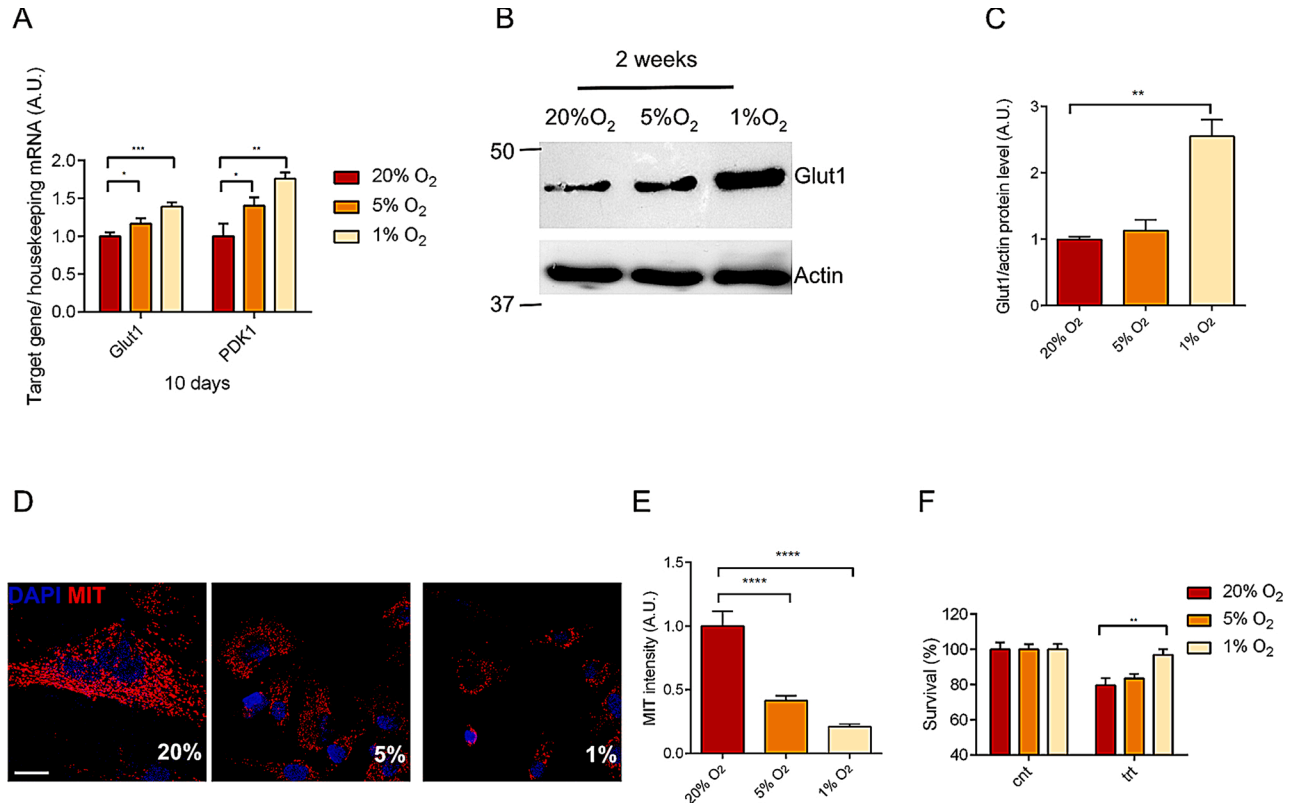

Fig. 4. Metabolism and resistance to stress of hAFSCs at different oxygen tensions. A) Transcript levels of Glut1 and PDK1 in hAFSCs cultivated at 20%, 5% and 1% oxygen tension. Actin and tubulin were used as housekeeping. *p value < 0.05; **p value < 0.01; ***p value < 0.001. B-C) Glut1 protein expression after 2 weeks of in vitro culture at different oxygen tensions. Actin was used as loading control. **p value < 0.01. D) hAFSCs cultivated at 20%, 5% and 1% oxygen tension were stained with anti-human MIT (red). Nuclei were visualized with DAPI (blue). Scale bar =10 μm. E) Relative normalized expression of corrected total cell fluorescence of h-MIT staining. ****p value < 0.001 F) Relative normalized viability of hAFSCs cultivated at 20, 5 or 1% oxygen tension after thapsigargin treatment. Viability of treated samples was normalized on the corresponding control cultivated at the same oxygen tension measured through MTS test. **p value < 0.01. A.U.= arbitrary units. Numeric data are presented as Mean +/- SEM. Data were obtained analysing at least two of the four patients in each experiment.

Since metabolic perturbations lead to altered mitochondrial structure (Solaini et al., 2010), we measured the number and the morphology of mitochondria by we staining cells with an antibody against a non-glycosylated protein component of mitochondria membrane surface (MIT). In cells at 1% O_2 mitochondria were less numerous and more fragmented compared to cells at 20 % O_2, with cells at 5% O_2 showing an intermediate phenotype (Fig. 4D-E).

Mitochondria are important sources of pro-apoptotic stimuli, and cells in hypoxia, in particular cancer cells, result more protected from stimuli inducing cell death (Nagaraj et al., 2007).

When we treated hAFSCs with thapsigargin, an inducer of endoplasmic reticulum stress, we observed a significant increase in viability in the cell population cultured at 1% O_2 (Fig. 4F). These data suggest that hAFSCs cultured under hypoxia adopt an altered metabolic profile that protect from pro-apoptotic stimuli.

2.5. *Hypoxia helps to maintain youthful differentiation potential*

Since hypoxia seemed to provide stemness, proliferative and metabolic advantages, we decided to evaluate the effect of low oxygen tension on differentiation properties. In particular, we focused on the balance between adipogenic and osteogenic differentiation, a process particularly relevant in aging (Bethel et al., 2020). whereas adipogenesis increases and osteoblastogenesis declines (Justesen et al., 2001). Adipogenesis relies on the activation of the transcription factor CEBPα which subsequently induces PPARγ, a receptor necessary to regulate the deposit of fatty acids and glucose metabolism in adipocytes (Kim and Chen, 2004).

Osteogenesis is initially regulated by the transcription factor RUNX2, which expression is then reduced during later phases when the matrix extracellular proteins osteopontin (encoded by the gene SPP1) and osteocalcin (encoded by the gene BGLAP) are deposited (Bruderer et al., 2014).

Upon exposure to an adipogenic differentiation medium, cells at lower oxygen concentrations displayed reduced expression levels of CEBPα and PPARγ, thus suggesting decreased adipogenic differentiation in comparison to cells at 20 % O_2 (Fig. 5A). Moreover, quantitative absorbance analysis of Oil Red staining showed that cells maintained at 20 % O_2 deposited more droplets compared to low oxygen conditions (Fig. 5B-Figure S5A).

In contrast, when exposed to an osteogenic medium, cells at lower oxygen concentrations, in particular at 1% O_2, showed increased levels of SPP1 and BGLAP, but not of RUNX2, suggesting the achievement of terminal differentiation (Fig. 5C). These results were confirmed by Alizarin-Red, which revealed a more extensive calcium matrix deposit in cells differentiated at 5 and 1% O_2 (Fig. 5D-Figure S5B).

These finding show that hAFSCs cultured at low oxygen concentrations preferentially differentiate into bone tissue, suggesting prolonged maintenance of youthful differentiation properties.

3. Discussion

Understanding the molecular processes controlling stem cell survival, self-renewal, quiescence, proliferative expansion and commitment to specific differentiated cell lineages is essential to uncover the drivers and effectors of age-associated stem cell dysfunction and to ameliorate their manipulation prior their use in clinic.

Aged stem cells accumulate toxic metabolites which can lead to DNA

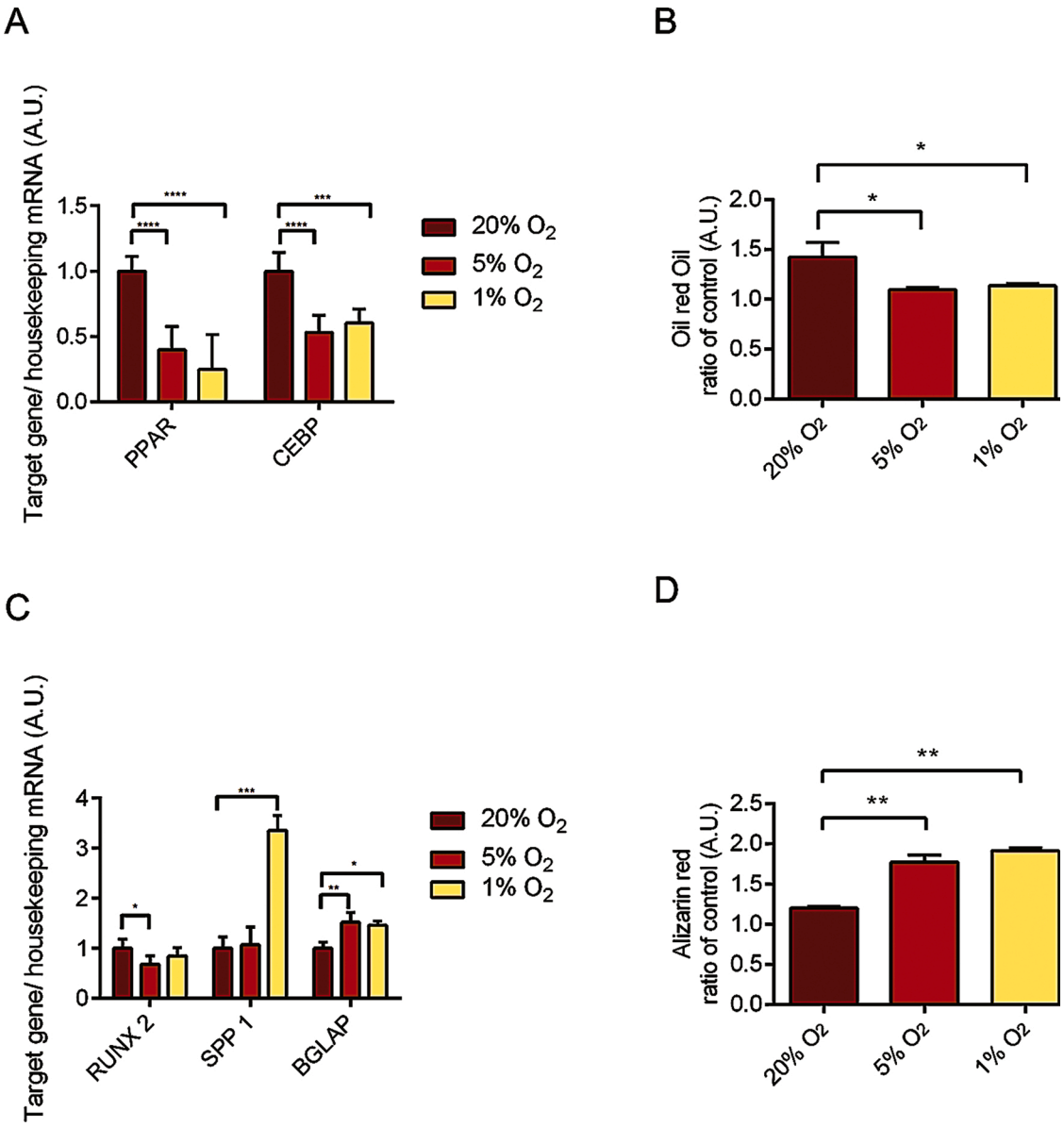

Fig. 5. Adipogenic and osteogenic differentiation potential of hAFSCs cultivated at different oxygen tensions. A) qPCR analysis for adipogenic markers (PPAR and CEBP) are reported. Actin and tubulin were used as housekeepers. ***p value < 0.001; ****p value < 0.001. B) Analysis of absorbance of Oil Red Staining in cells not differentiated (T_0) or after 21 days of adipose differentiation (diff). *p value<0.05. C) qPCR analysis for osteogenic markers (RUNX2, SPP1 and BGLAP) are reported. Actin and tubulin were used as housekeepers. *p value<0.05, **p value < 0.01, ***p value < 0.001. D)Analysis of absorbance of Alizarin Red Staining in cells not differentiated (T0) or after 21 days of osteogenic differentiation (diff). **p value < 0.01. A.U.= arbitrary units. Numeric data are presented as Mean +/- SEM. In both cases samples from two different patients were analysed.

and protein damage, mitochondrial dysfunction, proliferative exhaustion, chronic inflammation and epigenetic remodelling (Oh et al., 2014). In particular, oxidative stress is known to play an important role in modulating different stem cells properties, such as self-renewal, proliferation, differentiation and senescence (Guo et al., 2010). A potential major source of oxidative stress and accelerated aging of stem cells is the exposure to oxygen tensions higher than the concentration present in their natural niche (Jauniaux et al., 1999).

For this reason, the influence of oxygen tension on the morphology, phenotype, proliferative capacity, and functionality of adult stem cells, such as MSCs, has been increasingly studied.

Hypoxic conditions (1–10 % oxygen) seem sufficient to improve stem cells regenerative and proliferative properties, and to modulate their differentiation (Cruz and Rocco, 2015; Fehrer et al., 2007). The study from Schiavo et al. (2015) suggested that maintaining oxygen tension at 5% O_2 during both isolation and expansion of $CD117^+$ hAFSCs cells positively modulated proliferation and differentiation towards endothelium. However, this study completely avoided exposure to 20 % O_2 which would not fit with the actual routine practice to collect hAFSCs. Indeed, amniotic fluid cells of second trimester are normally cultured in cytogenetic laboratories and after 15 days at atmospheric oxygen tension the discarded flask is dedicated to research purpose and stem bank. Therefore, we decided to assess whether lower oxygen concentrations could improve the stemness and the replicative potential of hAFSCs isolated by standard procedures. We cultivated hAFSCs cells at 20 %, 5% and 1% O_2 for a period of 5 weeks. In general, major differences were observed among 1% O_2 and the other two conditions, where cells cultivated at 5% O_2 showed intermediate characteristics. The different results between 5% and 1% O_2 could be due to the different ability of these two oxygen tensions to induce metabolic changes in cells that normally reside in niches with very low oxygen tensions (Bertin et al., 2016). In fact, while 1% O_2 cells showed mitochondrial fragmentation

accompanied by expression of Glut1 and PDK1, two essential regulators of glycolysis, cells at 5% oxygen tension maintained more numerous mitochondria and less activation of Glut1 and PDK1.

The stemness marker Oct4 was upregulated in cells maintained at 1% O_2 compared to the other two conditions already after the first week in culture, contrasting with results obtained by Dionigi et al. who sustained that no differences in the expression of Oct4 mRNA could be appreciated between hAFSCs cultivated at 20 % O_2 or after seven days of hypoxia (Dionigi et al., 2014). This result was accompanied by a prolonged proliferative potential and the extension of cellular lifespan.

It has been reported that hypoxic conditions activate PI3K/Akt axis in bone marrow derived mesenchymal stem cells, enhancing their proliferation (Sheng et al., 2017) and the wound healing ability of their conditioned medium (Jun et al., 2014). The ratio of pAkt/Akt was increased in cells at 1% O_2, suggesting a role for this signalling pathway in maintaining proliferative capacity.

We have previously shown that the expression of pluripotency genes and the proliferation rate of hAFSCs are inversely correlated with the content of ROS, DNA damage and the onset of premature aging markers, including accumulation of prelamin A, the lamin A immature form, and large PML bodies (Casciaro et al., 2018). Cells at 1% O_2 showed lower expression of senescence-associated markers, such as p21, prelamin A and PML bodies, as well as β-galactosidase positivity, corroborating the idea that low oxygen tension preserves stemness properties and delays aging features.

It has been described that hypoxia (0.1–2% O_2) increases the viability of stem cells, both in normal culture conditions or under the effect of stressor molecules, by reducing apoptotic rates (Choi et al., 2014; Korski et al., 2019). For example, c-Kit$^+$ cardiac progenitor cells (hCPCs) are more viable after treatment with hydrogen peroxide (H_2O_2) if maintained at low oxygen tension [Korski et al., 2019). However, H_2O_2 activity is dependent on the presence of oxygen (Stadtman, 2006), and its activity is reduced at low oxygen. In this study, we demonstrated that hAFSCs cultivated at 1% O_2 are protected from apoptosis induced by stress that do not rely on oxygen concentrations, such as endoplasmic reticulum stress.

Ex vivo expansion of stem cells is an essential step to generate sufficient material suitable for therapeutic purposes. However, prolonged culture and activation of age-associated features can bias stem cells differentiation capacity. In the bone marrow niche, with progressive aging MSCs decrease osteogenesis and increase adipogenesis, a process thought to promote onset and progression of osteoporosis (Coipeau et al., 2009; Bethel et al., 2020). Hypoxia improves endothelial differentiation ability of hHFSCs (Lloyd-Griffith et al., 2015), but few information are available about differentiation towards mesenchymal commitment (Kwon et al., 2017). For this reason, we evaluated osteogenic and adipogenic differentiation potential of hAFSCs at different O_2, and showed that cells cultured at lower oxygen concentrations maintained increased osteogenic but reduced adipogenic commitment capability. This observation will be further validated in future *in vivo* studies.

In conclusion, our data suggest that maintaining human amniotic fluid stem cells at physiologically hypoxic oxygen tensions, more similar to their *in vivo* environment, preserves their function and delays the onset of aging features also after long-term expansion. These more physiological conditions might help to understand their biology, but also to facilitate their *ex vivo* expansion for therapeutic use in regenerative medicine.

4. Materials and methods

4.1. Amniotic fluid collection

Human amniotic fluid stem cells were obtained from 4 amniotic fluids collected from women between the 16th and 17th week of gestation during the amniocentesis procedure performed at Policlinico Hospital of Modena (Italy). The informed consent was obtained in accordance with the Italian law and the guidelines of the ethics committee (protocol 360/2017 dated 12.15.2017 approved by Area Vasta Emilia Nord).

The flasks of amniotic fluid cells were cultured in the Laboratory of Genetics of TEST Lab (Modena, Italy) for 2 weeks, then the supernumerary (unused) one was used for experiments.

4.2. Amniotic fluid stem cells selection

Human amniotic fluid stem cells (hAFSCs) were isolated as previously described by De Coppi et al. 2007 from not pathological donors (De Coppi et al., 2007). Human amniocentesis cultures were harvested by trypsinization and subjected to c-Kit immunoselection by MACS technology (Miltenyi Biotec, Germany). C-kit$^+$ positive cells represented about 5% of the total cellular population for each patient.

4.3. Cellular culture

hAFSCs were cultivated in MEM α GlutaMAX™ (Thermo Fisher Scientific, Vantaa, Finland) supplemented of 20 % foetal bovine serum (FBS) (GE Healthcare, Buckinghamshire, UK), 1% penicillin/streptomycin (Lonza, Basel, Switzerland), and kept in different incubators at 37 °C 5% CO_2 at 20 %, 5% or 1% oxygen.

hAFSCs were subcultured routinely at 1:3 dilution at the same time for all oxygen conditions and not allowed to expand beyond the 70 % of confluence. Approximately, cells used for experiments were at at culture passage reported in the follow table:

Experimental week	Culture passage
1 week	Passage 1
2 weeks	Passage 2–3
3 weeks	Passage 4–5
4 weeks	Passage 6–7
5 weeks	Passage 8–9

4.4. Differentiation assays

For each differentiation experiment, 50,000 cells were seeded in a P60 culture dish and kept in culture medium for 4 days. Then, the medium was replaced by differentiating media.

Osteogenic differentiation was obtained after 3 weeks of culture in a medium composed MEM α GlutaMAX™ (Thermo Fisher Scientific, Vantaa, Finland) with 10 % FBS (GE Healthcare, Buckinghamshire, UK), 1% penicillin/streptomycin (Lonza, Basel, Switzerland), 100 μM 2P-ascorbic acid, 100 nM dexamethasone and 10 mM β-glycerophosphate (all from Sigma-Aldrich, St Louis, MO, USA). The medium was changed twice a week.

For adipogenic differentiation, cells were incubated for 3 days in adipogenic induction medium composed by high glucose DMEM culture medium (Thermo Fisher Scientific, Vantaa, Finland) supplemented with 10 % FBS (GE Healthcare, Buckinghamshire, UK), 1% penicillin/streptomycin (Lonza, Basel, Switzerland), isobutylmethylxanthine, 1 μM dexamethasone, 10 μg/mL insulin, 0,2 mM indomethacin (all from Sigma-Aldrich, St Louis, MO, USA). After 3 days, the medium was replaced with one containing only 10 % FBS, 2 mM L-glutamine, 100 U/mL penicillin and 100 μg/mL streptomycin and 10 μg/mL insulin. It was changed twice a week and cells were kept in these conditions for 3 weeks.

After 3 weeks of osteogenic or adipogenic induction, the expression of specific lineage markers was evaluated through qRT-PCR as reported below.

4.5. Cellular viability

Cellular viability was evaluated using MTS assay. Cells were seeded at density of 3000 cell/well in a black 96 well plate, treated as reported in the paragraph "Cells treatments" and incubated with CellTiter 96® AQueous One Solution Cell Proliferation Assay (Promega Corporation, Madison, WI, USA), following the instructions of the producer.

The absorbance was measured on Promega multi well plate reader (Promega Corporation, Madison, WI, USA) at 450 nm.

4.6. EdU proliferation assay

Cellular proliferation was evaluated using EdU method. Cells were seeded at 8000 cells on coverslips put in a 24 multi well plate.

After 48 h, 10 μM EdU was added into the medium and cells were cultivated in these conditions for other 24 h. The day after, cells were fixed using 4% formaldehyde in PBS, kept 5 min in 100 mM Tris (pH 7.6), permeabilized 10 min in PBS + 0.1 % Triton X-100, washed in PBS and incubated with a PBS label mix containing 2 mM Cu(II)SO_4, 4 μM sulfo-Cy3-azide, 20 mg/mL sodium ascorbate for 30 min in the dark. After washing cells with PBS three times for five minutes each, coverslips were mounted with mounting media (including DAPI to visualize nuclei) onto glass slides and visualized at fluorescent microscope.

4.7. Senescence assay

In order to evaluate the presence of senescent cells in hAFSC samples, 10,000 cells/well were seeded in 24-well plates and after two days were fixed and processed as reported by Dimri et al. (Dimri et al., 1995).

The positivity was directly evaluated at the optical microscope EVOS XL Core Cell Imaging System (Thermo Fisher Scientific, Vantaa, Finland).

4.8. Cellular morphology

Cellular images were acquired using EVOS XL Core Cell Imaging System (Thermo Fisher Scientific, Vantaa, Finland). Parameter and area were measured with ImageJ using images pixels as scale. Cellular elongation was calculated using the following formula:

$$\text{Cellular elongation} = p^2 / 4\pi * A$$

where p is the cellular perimeter, π is equivalent to 314 and A represents the cellular area.

4.9. Cells treatments

Cells were seeded at 4000/wells in a 96 multi well plate and treated with 100 nM thapsigargin (Sigma-Aldrich, St Louis, MO, USA) for 24 h.

4.10. Cellular extracts preparation

Cell extracts were obtained as described by Maraldi et al. (Maraldi et al., 2015). Briefly, subconfluent cells were extracted by addition of AT lysis buffer (20 mM Tris-Cl, pH 7.0; 1% Nonidet P-40; 150 mM NaCl; 10 % glycerol; 10 mM EDTA; 20 mM NaF; 5 mM sodium pyrophosphate; and 1 mM Na_3VO_4) and freshly added Sigma Aldrich Protease Inhibitor Cocktail at 4 °C for 30 min. Lysates were sonicated, cleared by centrifugation and immediately boiled in SDS sample buffer.

4.11. SDS PAGE and western blot

Whole cell lysates from hAFSCs were processed as previously described (Zavatti et al., 2013). Primary antibodies were raised against the following molecules: Rabbit-Actin (Sigma-Aldrich, St Louis, MO, USA), Goat-Akt (Santa Cruz Biotechnology, CA, USA), Rabbit-p473Akt (Cell Signaling Technology, MA, USA), Mouse-Oct4 (Santa Cruz Biotechnology, CA, USA), Mouse-Cyclin A (Cell Signaling Technology, MA, USA), Rabbit-Cyclin B1 (Cell Signaling Technology, MA, USA), Cyclin E2 (Cell Signaling Technology, MA, USA), Rabbit-Glut1 (Millipore, CA, USA), Rabbit-p16 (Abcam, Cambridge, UK), Rabbit-p21 (Cell Signaling Technology, MA, USA).

Secondary antibodies, used at 1:3000 dilution, were all from Thermo Fisher Scientific (Waltham, MA, USA).

4.12. Immunofluorescence and confocal microscopy

For immunofluorescence analyses, 15,000 cells/well were seeded in coverslips put in 24 multi well plates and processed as previously described (Guida et al., 2013). Confocal imaging was performed by a Nikon A1 confocal laser scanning microscope, as previously described (Maraldi et al., 2016). Primary antibodies were raised against the following molecules: Rabbit-Prelamin A (Diatheva, Fano, PU, Italy), Mouse-PML (Santa Cruz Biotechnology, CA, USA), Goat-Ki67 (Santa Cruz Biotechnology, CA, USA), Mouse-Human MIT (Millipore, CA, USA), Mouse-SSEA-4 (Cell Signaling, MA, USA), Mouse-TRA1−81 (Santa Cruz Biotechnology, CA, USA), Goat-CD29 (Santa Cruz Biotechnology, CA, USA), Rabbit-CD44 (Santa Cruz Biotechnology, CA, USA), Rabbit-CD73 (GeneTex CA, USA), Mouse-CD90(Millipore, CA, USA), Mouse-CD105 (Millipore CA, USA), following datasheet instructions.

Alexa secondary antibodies (Thermo Fisher Scientific, Waltham, MA, USA) were used at 1:200 dilution.

4.13. RT-PCR

Cells were seeded at 2000 cells/cm2 density and kept in culture for 3 days. After this time, total RNA was isolated using the Isolate II RNA Mini Kit (Bioline Meridian Bioscience, Paris, France), following producer instructions. 500 ng of RNA were reverse transcribed into cDNA using the kit High Capability cDNA Reverse Transcription (Applied Biosystems, Waltham, MA, USA). The reaction was accomplished in a T100™ Thermal Cycler (Bio-rad, Hercules, CA, USA).

The obtained cDNA samples were diluted at 5 ng/μl and 12 ng of each sample were loaded to perform qRT-PCR using the Universal Probe Library system (Roche, Basel, Switzerland) and SENSIFast Probe kit (Bioline Meridian Bioscience, Paris, France). The reaction was carried out using the LightCycler® 480 Instrument II (Roche, Basel, Switzerland) in a 360 PCR multi well plate. Analysis of tubulin and actin were used to normalize the expression of other genes CT values.

The list of primers used in these experiments is reported below.

Gene	Sequence	RefSeq accession n
hNANOG	Fw cagtctggacactggctgaa Rv cacgtggtttccaaacaaga Probe 55	NM_024865
hPOU5F1 (Oct4)	Fw tgagtagtcccttcgcaagc Rv gagaaggcgaaatccgaag Probe 60	NM_002701.5
hCDKN2A (p16)	Fw gagcagcatggagccttc Rv cgtaactattcggtgcgttg Probe 67	NM_000077.4
hCDKN1A (p21)	Fw tcactgtcttgtacccttgtgc Rv ccgttttcgaccctgagag Probe 32	NM_000389.4
hSLC2A1 (Glut1)		NM_006516.2
hPDK1	Fw tcctttgaatctaagtatttgtttcct Rv catttttccttttaaaacatttcttagc Probe 52	NM_001278549.1
hCCNE2 (cyclin E2)	Fw ccccaagaagcccagataat Rv caggtggccaacaattcct Probe 35	NM_057749.2
hPPARG	Fw gacctgaaacttcaagagtaccaaa Rv tgaggcttattgtagagctgagtc Probe 39	NM_138712
hCEBPA		NM_001285829.1

(continued on next page)

(*continued*)

Gene	Sequence	RefSeq accession n
	Fw gacatcagcgcctacatcg Rv ggctgtgctggaacaggt Probe 72	
hRUNX2	Fw cagtgacaccatgtcagcaa Rv gctcacgtcgctcattttg Probe 41	NM_001015051
hSPP1 (Osteopontin)	Fw gggcttggttgtcagcag Rv tgcaattctcatggtagtgagttt Probe 63	NM_001251830
hBGLAP (Osteocalcin)	Fw tgagagccctcacactcctc Rv acctttgctggactctgcac Probe 81	NM_199173
SMARCC1(Baf155)	Fw gtgtcccagctggattcg Rv agcatccgcatgaacatactt Probe 61	NM_003074.3
RCOR2	Fw cacccaccctgattggaa Rv gacgtcagggctcagagtg Probe 50	NM_173587.3
ZNF219 (ZFP219)	Fw tctctggcttccctgcac Rv caacagcccattctcttcct Probe 57	NM_016423.2
ZNF462 (ZFP462)	Fw caatttgaaggagaccactgc Rv aaccacagggtctggcatt Probe 68	NM_021224.5
SOX2	Fw ttgctgcctctttaagactagga Rv taagcctggggctcaaact Probe 35	NM_003106.3
RIF1	Fw aactcaaagcttgatgaagttccta Rv gctgaattgcagacaagcaata Probe 14	NM_018151.4
hTUBULIN	Fw cttcgtctccgccatcag Rv cgtgttccaggcagtagagc Probe 40	NM_006009.3
hACTB	Fw ccaaccgcgagaagatga Rv ccagaggcgtacagggatag Probe 64	NM_001101.3

4.14. Oct4 activity

Oct4 binding activity was detected using the colorimetric Oct4 Transcription Factor Assay (Abcam). Briefly, cells nuclear proteins were collected using the Nuclear extraction Kit (Abcam) and quantified using a BCA Protein Assay Kit (Thermo Fisher Scientific). Twenty micrograms of nuclear extracts were added to pre-coated wells containing Oct4 consensus binding site and incubated with Oct4 primary antibody (Abcam) followed by incubation with HRP-conjugated secondary antibody (Abcam). Five micrograms of P19 nuclear extract was used as positive controls. Absorbance was detected at OD 450 using a plate reader according manufacturer's instruction (Glomax-multi Detection System).

4.15. Oil red-O staining

Briefly undifferentiated and differentiated cells were washed with PBS and fixed with 4% paraformaldehyde for 15 min at room temperature. After fixation and additional washes, the cells were incubated with Oil red Oil solution (Sigma-Aldrich, St Louis, MO, USA) in 40 % isopropanol and images were captured under light microscope. Oil red-O was extracted from three replicates with 100 % isopropyl alcohol and its absorbance measured by Promega multi well plate reader (Promega Corporation, Madison, WI, USA) at 510 nm (Pazienza et al., 2014).

4.16. Alizarin Red S staining and mineralization

Fixed monolayer cells were washed with distilled water and then incubated with a 2% of Alizarin Red S solution (Abcam, Cambridge, UK) at pH 4.2 for 10 min at RT. Images of samples were obtained with a EVOS XL Core Cell Imaging System microscope (Thermo Fisher Scientific, Vantaa, Finland).

To quantify the Alizarin Red S staining, stained samples were washed three times with PBS and then 1 mL of 10 % cetylpyridinium chloride was added to each well and incubated for 20 min to elute the stain. 100 µL of this eluted stain were added to 96 well plates and absorbance read at 485 nm using a multi well plate reader (Promega Corporation, Madison, WI, USA) (Zavatti et al., 2013).

4.17. Statistical analysis

In vitro experiments were performed in triplicate. For quantitative comparisons, values were reported as mean ± SEM based on triplicate analysis for each sample. To test the significance of observed differences among the study groups One-way Anova test was applied when just a time point was evaluated, while Two-way Anova was performed when more time points were taken in consideration. A P value <0.05 was considered to be statistically significant. Statistical analysis and plot layout were obtained by using GraphPad Prism® release 6.0 software.

Author disclosure statement

All the authors report no conflict of interest since nobody has commercial associations that might create a conflict of interest in connection with the submitted manuscript.

Authors' contributions

FC, performed, acquired and interpreted experimental data and drafted the manuscript; MB, acquired experimental data and revised the manuscript; FB, acquired experimental data; MZ and EB, derived amniotic fluid stem cells; MYF, revised the manuscript; TM, acquired and interpreted experimental data and drafted the manuscript; MD, designed and supervised the study and wrote the manuscript. All authors read and approved the final manuscript.

Ethics approval and consent to participate

An informed consent allowing the use of clinical data and biological samples for the specified research purpose (protocol 360/2017 dated 12.15.2017 approved by Area Vasta Emilia Nord) was signed by all infertile couples before treatment and collected by the Unit of Obstetrics & Gynecology, Policlinico Hospital of Modena (Italy).

Consent for publication

Not applicable since the manuscript does not contain any individual person's data in any form.

Acknowledgments

This work was supported by grants from the Dutch Cancer Foundation (KWF) and from the University Medical Center Groningen (UMCG) to M.D.

Appendix A. Supplementary data

Supplementary material related to this article can be found, in the online version, at doi:https://doi.org/10.1016/j.mad.2020.111328.

References

Antoniou, E.S., Sund, S., Homsi, E.N., Challenger, L.F., Rameshwar, P., 2004. A theoretical simulation of hematopoietic stem cells during oxygen fluctuations: prediction of bone marrow responses during hemorrhagic shock. Shock 22 (5), 415–422. Accessed April 2, 2019. http://www.ncbi.nlm.nih.gov/pubmed/15489633.

Antonucci, I., Di Pietro, R., Alfonsi, M., et al., 2014. Human second trimester amniotic fluid cells are able to create embryoid body-like structures in vitro and to show typical expression profiles of embryonic and primordial germ cells. Cell Transplant. 23 (12), 1501–1515. https://doi.org/10.3727/096368914X678553.

Bertin, E., Piccoli, M., Franzin, C., et al., 2016. First steps to define murine amniotic fluid stem cell microenvironment. Sci. Rep. 6 (1), 37080. https://doi.org/10.1038/srep37080.

Bethel, M., Chitteti, B.R., Srour, E.F., 2020. Rohn Professor of Leukemia Research AS, Kacena MA, Professor a. The Changing Balance Between Osteoblastogenesis and Adipogenesis in Aging and Its Impact on Hematopoiesis doi:10.1007/s11914-013-0135-6.

Bruderer, M., Richards, R.G., Alini, M., Stoddart, M.J., 2014. Role and regulation of RUNX2 in osteogenesis. Eur. Cell. Mater. 28, 269–286. Accessed June 26, 2019. http://www.ncbi.nlm.nih.gov/pubmed/25340806.

Cananzi, M., De Coppi, P., 2012. CD117+ amniotic fluid stem cells: state of the art and future perspectives. Organogenesis 8 (3), 77–88. https://doi.org/10.4161/org.22426.

Casciaro, F., Beretti, F., Zavatti, M., et al., 2018. Nuclear Nox4 interaction with prelamin A is associated with nuclear redox control of stem cell aging. Aging (Albany NY) 10 (10), 2911–2934. https://doi.org/10.18632/aging.101599.

Choi, J.R., Pingguan-Murphy, B., Abas, W.A.B.W., et al., 2014. Hypoxia promotes growth and viability of human adipose-derived stem cells with increased growth factors secretion. J Asian Sci Res. 4 (7), 328–338. Accessed April 28, 2019. https://econpapers.repec.org/article/asijoasrj/2014_3ap_3a328-338.htm.

Coipeau, P., Rosset, P., Langonne, A., et al., 2009. Impaired differentiation potential of human trabecular bone mesenchymal stromal cells from elderly patients. Cytotherapy 11 (5), 584–594. https://doi.org/10.1080/14653240903079385.

Cruz, F.F., Rocco, P.R.M., 2015. Hypoxic preconditioning enhances mesenchymal stromal cell lung repair capacity. Stem Cell Res. Ther. 6 (1), 130. https://doi.org/10.1186/s13287-015-0120-3.

Davalli, P., Mitic, T., Caporali, A., Lauriola, A., D'arca, D.R.O.S., 2016. Cell Senescence, and Novel Molecular Mechanisms in Aging and Age-Related Diseases. https://doi.org/10.1155/2016/3565127.

De Coppi, P., Bartsch, G., Siddiqui, M.M., et al., 2007. Isolation of amniotic stem cell lines with potential for therapy. Nat. Biotechnol. 25 (1), 100–106. https://doi.org/10.1038/nbt1274.

Dimri, G.P., Lee, X., Basile, G., et al., 1995. A biomarker that identifies senescent human cells in culture and in aging skin in vivo. Proc Natl Acad Sci 92 (20), 9363–9367. https://doi.org/10.1073/pnas.92.20.9363.

Dionigi, B., Ahmed, A., Pennington, E.C., Zurakowski, D., Fauza, D.O., 2014. A comparative analysis of human mesenchymal stem cell response to hypoxia in vitro: implications to translational strategies. J. Pediatr. Surg. 49 (6), 915–918. https://doi.org/10.1016/j.jpedsurg.2014.01.023.

Ermolaeva, M., Neri, F., Ori, A., Lenhard Rudolph, K., 2018. Cellular and Epigenetic Drivers of Stem Cell Ageing. https://doi.org/10.1038/s41580-018-0020-3.

Estrada, J.C., Albo, C., Benguría, A., et al., 2012. Culture of human mesenchymal stem cells at low oxygen tension improves growth and genetic stability by activating glycolysis. Cell Death Differ. 19 (5), 743–755. https://doi.org/10.1038/cdd.2011.172.

Fehrer, C., Brunauer, R., Laschober, G., et al., 2007. Reduced oxygen tension attenuates differentiation capacity of human mesenchymal stem cells and prolongs their lifespan. Aging Cell 6 (6), 745–757. https://doi.org/10.1111/j.1474-9726.2007.00336.x.

Gao, Z., Zhu, X., Dou, Y., 2015. The miR-302/367 cluster: a comprehensive update on its evolution and functions. Open Biol. 5 (12), 150138. https://doi.org/10.1098/rsob.150138.

Gardner, L.B., Li, Q., Park, M.S., Flanagan, W.M., Semenza, G.L., Dang, C.V., 2001. Hypoxia Inhibits G_1 /S Transition through Regulation of p27 Expression. J. Biol. Chem. 276 (11), 7919–7926. https://doi.org/10.1074/jbc.M010189200.

Grayson, W.L., Zhao, F., Izadpanah, R., Bunnell, B., Ma, T., 2006. Effects of hypoxia on human mesenchymal stem cell expansion and plasticity in 3D constructs. J. Cell. Physiol. 207 (2), 331–339. https://doi.org/10.1002/jcp.20571.

Greer Card, D.A., Hebbar, P.B., Li, L., et al., 2008. Oct4/Sox2-regulated miR-302 targets cyclin D1 in human embryonic stem cells. Mol. Cell. Biol. 28 (20), 6426–6438. https://doi.org/10.1128/MCB.00359-08.

Guida, M., Maraldi, T., Resca, E., et al., 2013. Inhibition of nuclear Nox4 activity by plumbagin: effect on proliferative capacity in human amniotic stem cells. Oxid. Med. Cell. Longev. 2013, 1–12. https://doi.org/10.1155/2013/680816.

Guo, Y.-L., Chakraborty, S., Rajan, S.S., Wang, R., Huang, F., 2010. Effects of oxidative stress on mouse embryonic stem cell proliferation, apoptosis, senescence, and self-renewal. Stem Cells Dev. 19 (9), 1321–1331. https://doi.org/10.1089/scd.2009.0313.

Hayflick, L., 1965. The limited in vitro lifetime of human diploid cell strains. Exp. Cell Res. 37 (3), 614–636. https://doi.org/10.1016/0014-4827(65)90211-9.

Hernandez-Segura, A., Nehme, J., Demaria, M., 2018. Hallmarks of cellular senescence. Trends Cell Biol. 28 (6), 436–453. https://doi.org/10.1016/j.tcb.2018.02.001.

Holzwarth, C., Vaegler, M., Gieseke, F., et al., 2010. Low physiologic oxygen tensions reduce proliferation and differentiation of human multipotent mesenchymal stromal cells. BMC Cell Biol. 11 (1), 11. https://doi.org/10.1186/1471-2121-11-11.

Jauniaux, E., Watson, A., Ozturk, O., Quick, D., Burton, G., 1999. In-vivo measurement of intrauterine gases and acid-base values early in human pregnancy. Hum. Reprod. 14 (11), 2901–2904. Accessed April 28, 2019. http://www.ncbi.nlm.nih.gov/pubmed/10548645.

Jun, E.K., Zhang, Q., Yoon, B.S., et al., 2014. Hypoxic conditioned medium from human amniotic fluid-derived mesenchymal stem cells accelerates skin wound healing through TGF-β/SMAD2 and PI3K/Akt pathways. Int. J. Mol. Sci. 15 (1), 605–628. https://doi.org/10.3390/ijms15010605.

Justesen, J., Stenderup, K., Ebbesen, E.N., Mosekilde, L., Steiniche, T., Kassem, M., 2001. Adipocyte tissue volume in bone marrow is increased with aging and in patients with osteoporosis. Biogerontology 2 (3), 165–171. Accessed June 20, 2019. http://www.ncbi.nlm.nih.gov/pubmed/11708718.

Kim, J.E., Chen, J., 2004. Regulation of peroxisome proliferator-activated receptor-activity by mammalian target of rapamycin and amino acids in Adipogenesis. Diabetes 53 (11), 2748–2756. https://doi.org/10.2337/diabetes.53.11.2748.

Kim, J.H., Kim, S.-H., Song, S.Y., et al., 2014. Hypoxia induces adipocyte differentiation of adipose-derived stem cells by triggering reactive oxygen species generation. Cell Biol. Int. 38 (1), 32–40. https://doi.org/10.1002/cbin.10170.

Korski, K.I., Kubli, D.A., Wang, B.J., et al., 2019. Hypoxia prevents mitochondrial dysfunction and senescence in human c-Kit $^{+}$ cardiac progenitor cells. Stem Cells 37 (4), 555–567. https://doi.org/10.1002/stem.2970.

Krishnamurthy, J., Ramsey, M.R., Ligon, K.L., et al., 2006. p16INK4a induces an age-dependent decline in islet regenerative potential. Nature 443 (7110), 453–457. https://doi.org/10.1038/nature05092.

Kwon, S.Y., Chun, S.Y., Ha, Y.-S., et al., 2017. Hypoxia enha cell properties of human mesenchymal stem cells. Tissue Eng Regen Med 14 (5), 595–604. https://doi.org/10.1007/s13770-017-0068-8.

Lee J., Go Y., Kang I., Han Y.-M., Kim J. Oct-4 controls cell-cycle progression of embryonic stem cells. 2010;426(2):171-181. doi:10.1042/BJ20091439.

Li, T.-S., Marbán, E., 2010. Physiological Levels of Reactive Oxygen Species are Required to Maintain Genomic StabiliT.-S.y in Stem Cells. Stem Cells 28 (7). https://doi.org/10.1002/stem.438. N/A-N/A.

Lloyd-Griffith, C., Duffy, G.P., O'Brien, F.J., 2015. Investigating the effect of hypoxic culture on the endothelial differentiation of human amniotic fluid-derived stem cells. J Anat 227 (6), 767–780. https://doi.org/10.1111/joa.12283.

Loukogeorgakis, S.P., De Coppi, P., 2016. Stem cells from amniotic fluid - Potential for regenerative medicine. Best Pract Res Clin Obstet Gynaecol 31, 45–57. https://doi.org/10.1016/j.bpobgyn.2015.08.009.

Lu, Y., Qu, H., Qi, D., et al., 2019. OCT4 maintains self-renewal and reverses senescence in human hair follicle mesenchymal stem cells through the downregulation of p21 by DNA methyltransferases. Stem Cell Res Ther 10 (1), 28. https://doi.org/10.1186/s13287-018-1120-x.

Maraldi, T., Guida, M., Zavatti, M., et al., 2015. Nuclear Nox4 Role in Stemness Power of Human Amniotic Fluid Stem Cells. Oxid Med Cell Longev 2015, 1–11. https://doi.org/10.1155/2015/101304.

Maraldi, T., Resca, E., Nicoli, A., et al., 2016. NADPH oxidase-4 and MATER expressions in granulosa cells: Relationships with ovarian aging. Life Sci 162, 108–114. https://doi.org/10.1016/J.LFS.2016.08.007.

Mulyawan, I.M., 2019. Role of Ki67 protein in colorectal cancer. Int J Res Med Sci 7 (2), 644. https://doi.org/10.18203/2320-6012.ijrms20190374.

Nagaraj, N.S., Vigneswaran, N., Zacharias, W., 2007. Hypoxia inhibits TRAIL-induced tumor cell apoptosis: Involvement of lysosomal cathepsins. Apoptosis 12 (1), 125–139. https://doi.org/10.1007/s10495-006-0490-1.

Oh, J., Lee, Y.D., Wagers, A.J., 2014. Stem cell aging: mechanisms, regulators and therapeutic opportunities. Nat Med 20 (8), 870–880. https://doi.org/10.1038/nm.3651.

Pazienza, V., Borghesan, M., Mazza, T., et al., 2014. SIRT1-metabolite binding histone macroH2A1.1 protects hepatocytes against lipid accumulation. . Aging (Albany NY) 6 (1), 35–47. https://doi.org/10.18632/aging.100632.

Pezzi, A., Amorin, B., Laureano, Á, et al., 2017. Effects Of Hypoxia in Long-Term In Vitro Expansion of Human Bone Marrow Derived Mesenchymal Stem Cells. J Cell Biochem 118 (10), 3072–3079. https://doi.org/10.1002/jcb.25953.

Roubelakis, M.G., Pappa, K.I., Bitsika, V., et al., 2007. Molecular and Proteomic Characterization of Human Mesenchymal Stem Cells Derived from Amniotic Fluid: Comparison to Bone Marrow Mesenchymal Stem Cells. Stem Cells Dev 16 (6), 931–952. https://doi.org/10.1089/scd.2007.0036.

Salomoni, P., Pandolfi, P.P., 2002. The role of PML in tumor suppression. Cell 108 (2), 165–170. Accessed April 10, 2019. http://www.ncbi.nlm.nih.gov/pubmed/11832207.

Sheng, L., Mao, X., Yu, Q., Yu, D., 2017. Effect of the PI3K/AKT signaling pathway on hypoxia-induced proliferation and differentiation of bone marrow-derived mesenchymal stem cells. Exp Ther Med 13 (1), 55–62. https://doi.org/10.3892/etm.2016.3917.

Solaini, G., Baracca, A., Lenaz, G., Sgarbi, G., 2010. Hypoxia and mitochondrial oxidative metabolism. Biochim Biophys Acta - Bioenerg 1797 (6-7), 1171–1177. https://doi.org/10.1016/j.bbabio.2010.02.011.

Stadtman, E.R., 2006. Protein Oxidation in Aging and Age-Related Diseases. . Ann N Y Acad Sci 928 (1), 22–38. https://doi.org/10.1111/j.1749-6632.2001.tb05632.x.

Ullah, I., Subbarao, R.B., Rho, G.J., 2015a. Human mesenchymal stem cells - current trends and future prospective. Biosci Rep 35 (2), 1–18. https://doi.org/10.1042/BSR20150025.

Ullah, I., Subbarao, R.B., Rho, G.J., 2015b. Human mesenchymal stem cells - Current trends and future prospective. Biosci Rep 35 (2). https://doi.org/10.1042/BSR20150025.

Valorani, M.G., Montelatici, E., Germani, A., et al., 2012. Pre-culturing human adipose tissue mesenchymal stem cells under hypoxia increases their adipogenic and osteogenic differentiation potentials. Cell Prolif 45 (3), 225–238. https://doi.org/10.1111/j.1365-2184.2012.00817.x.

van den Berg, D.L.C., Snoek, T., Mullin, N.P., et al., 2010. An Oct4-Centered Protein Interaction Network in Embryonic Stem Cells. Cell Stem Cell 6 (4), 369–381. https://doi.org/10.1016/j.stem.2010.02.014.

Wagegg, M., Gaber, T., Lohanatha, F.L., et al., 2012. Hypoxia Promotes Osteogenesis but Suppresses Adipogenesis of Human Mesenchymal Stromal Cells in a Hypoxia-Inducible Factor-1 Dependent Manner. Covas DT, ed. PLoS One. 7 (9), e46483. https://doi.org/10.1371/journal.pone.0046483.

Wang, S., Qu, X., Zhao, R., 2012. Clinical applications of mesenchymal stem cells. J Hematol Oncol 5 (1), 19. https://doi.org/10.1186/1756-8722-5-19.

Zavatti, M., Resca, E., Bertoni, L., et al., 2013. Ferutinin promotes proliferation and osteoblastic differentiation in human amniotic fluid and dental pulp stem cells. Life Sci 92 (20-21), 993–1003. https://doi.org/10.1016/J.LFS.2013.03.018.